Analysis of printing and writing papers by using direct analysis in real time mass spectrometry

Jeanette Adams *

Binding and Collections Care Division, Library of Congress, 101 Independence Ave., SE, Washington, DC 20540-4520, USA

A B S T R A C T

A quick and direct method for identifying organic components of papers in library and archival collections with minimal destructive sampling is needed for preservation, forensic, and general purposes. Direct analysis in real time mass spectrometry (DART-MS) is used for characterizing 16 reference papers of known manufacture in terms of their pulp composition and pitch contaminants. Unique mass spectra are obtained from bleached kraft, chemithermomechanical, and stone groundwood pulp papers in real time without extractions, derivatizations, chromatographic separations, and other time- and chemical-consuming sample preparations. Phytosteroids are volatilized from bleached hardwood kraft but not from bleached softwood kraft papers, which differentiates the two of them. The kraft papers are in turn differentiated from chemithermomechanical pulp papers by lignin-derived thermolyis products: syringyl products arise from hardwood, but guaiacyl and coumaryl products arise from softwood, chemithermomechanical pulp papers. Stone groundwood papers contain a number of extractives that are volatilized, which serve to differentiate them from all the other papers. Papers that contain rosin vs. alkyl ketene dimer (AKD) sizings are immediately differentiated. The DART-MS methodology is fast and simple, and the spectra are repeatable. Microsamples as small as ~10 μg tweezed from the paper surface may be analyzed. These benchmark spectra are the prelude to further applications of DART-MS in paper research and the beginning of the development of a searchable library of DART-MS spectra of printing and writing papers by the Library of Congress.

Published by Elsevier B.V.

1. Introduction

The chemical composition of printing and writing papers varies with manufacture and age [1–4]. Some of the most stable European papers were hand-made prior to approximately 1650 from high-quality linen rags. These papers contain long cellulose fibers, frequently have an alkaline pH from calcium and magnesium carbonates, and are impregnated with gelatin as an external sizing agent, which was used to either decrease or prevent ink from feathering when applied to the paper. During the latter half of the 17th century, mechanization and the newly born science of chemistry [5] began to play greater roles in paper production. Papermaker's alum (aluminum sulfate, $Al_2(SO_4)_3 \cdot 18H_2O$) began to be used to help set the gelatin sizing and improve the properties of the sheet, but it was not yet known that Al^{3+} would undergo hydrolysis in the presence of water to generate acidity ($pK_a = 5.0$) [4]. The Industrial Revolutions of the 18th and 19th centuries then gave rise to new papermaking machinery that severely macerated the pulp and

fast heat-dried the paper. This was coupled with the use of sulfuric acid and chlorine as bleaches; the substitution of rag fibers with straw, vegetable, and ultimately, in 1840s, mechanical stone groundwood; and the replacement of gelatin with alum-rosin internal sizing. Mechanical pulp fibers are short and unpurified so they contain high levels of lignin and other phytochemicals that are either inherently acidic, can decompose to produce acids, and/or can cause photoyellowing. Rosin sizing contains abietic and similar acids, and requires alum and an acidic pH for efficient sizing. Deterioration of the physicochemical properties of paper continued into the 20th century in spite of the invention of delignified chemical wood pulp and the introduction of calcium carbonate as a filler. During the late 20th century, alkaline papermaking using the synthetic sizing agents alkyl ketene dimer (AKD) and alkenyl succinic anhydride (ASA) and chlorine-free bleaching processes began to be used in response to environmental regulations and concerns about the archival permanence of paper. However, acidic papers that contain alum-rosin sizing continue to be produced around the world [6]. International movements toward green technology are setting targets for the use of high-yield chemithermomechanical and post-consumer recycled pulps in 21st century papers [7]. Consequently, the paper substrate that is the base material in library and archival written and printed collections is and will continue to be inherently

* Corresponding author. Tel.: +1 202 707 1031; fax: +1 202 707 3434.
  E-mail address: jead@loc.gov.

highly variable and subject to chemical degradation at variable rates.

Determining the various chemical components of different paper substrates and their impact on long-term physical and optical stability, and determining the impact of conservation treatments on the components, is a challenge. Although the acidity of paper is well accepted as having a major impact on stability, other chemical components including metal ions, lignin, additives, and degradation products, and effects of temperature, humidity, oxygen, light, and pollutants on the chemical components, also impact degradation [8]. Studies of historic naturally aged papers have provided useful insights into some degradation processes [2,9–11], but the original properties of the papers and the conditions under which they have been stored are variables that can impact their physicochemical properties in unknown ways. To reduce the variables, studies of modern reference papers of known manufacture are now being used more extensively in accelerated aging experiments to model aging behavior of naturally aged papers. These reference papers include one set made in the early 1990s for researchers in the European conservation community [12] and another set made in 1995 for the ASTM International Institute for Standards Research (ASTM-ISR) as part of the *ASTM Paper Aging Research Program* [13]. Aqueous and organic extracts of some of the ASTM-ISR papers, of which the Library of Congress is steward, were analyzed before and after accelerated aging, but the chromatographic methodologies were indirect and compound-class specific: capillary electrophoresis (CE) with either UV or photodiode array detection was used to detect low-mass water soluble aliphatic acids and either water- or methanol-soluble monomeric lignin degradation products; high performance liquid chromatography (HPLC) with UV detection was used to detect methanol-soluble monomeric lignin degradation products; ion chromatography with pulsed amperometric detection was used to detect low-mass water soluble sugars; and gas chromatography–mass spectrometry (GC–MS) was used to detect methyl-*t*-butyl ether soluble fatty and resin acids after silylation.

Other analytical methods have also been used to study paper. Fourier transform (FT) infrared, near infrared, and FT-Raman spectroscopy, with or without either spectral deconvolution or chemometric analysis, have been used to study paper degradation [14,15]. These non-destructive spectroscopic methods may reveal functional groups of predominant compounds but not specific compound identification. Pyrolysis GC (Py-GC) and Py-GC–MS have been used to analyze paper and additives with and without derivatization [16–20]. These micro-destructive methods provide for identification of compounds volatilized and/or formed by pyrolysis, but GC is limited by compound volatility and thermal stability, and the analyses are time consuming.

An analytical technique that provides fast sample throughput and identification of relevant organic compounds with minimal destructive sampling would be invaluable in paper research. Direct analysis in real time mass spectrometry (DART-MS) is a relatively new MS method that directly and quickly identifies intact volatile, semivolatile, and nonvolatile polar organic compounds in a variety of matrices without extractions, derivatizations, and chromatographic separations [21]. Analyses of solid samples have included writing inks [22], bacterial whole cells [23], flies [24], plant materials [25], and toys [26]. Several studies have addressed mechanisms of ion formation and factors that impact sensitivity and reproducibility [21,27–29].

This article is the first to describe methods to characterize printing and writing papers by using positive ion DART-MS. Whatman #1 100% cotton cellulose filter paper and the 15 ASTM-ISR reference papers were analyzed. Specific techniques that provide a thorough analysis, and the repeatability and sensitivity of the method for analyzing microsamples, are addressed. Positive ions observed by using DART-MS are discussed in relation to ions observed by using Py-MS, which provides added insight into ion formation from solid materials by using DART-MS.

2. Experimental

2.1. Instrumental analysis

The mass spectrometer used in these experiments is a JEOL JMS-T100 DART AccuTOF-D (JEOL USA, Peabody, MA) equipped with a second-generation DART ion source (IonSense, Saugus, MA). The pertinent settings for the interface between the pinhole orifice at atmospheric pressure and the low-pressure of the time-of-flight (TOF) mass analyzer were: Orifice One (O1), 30 V and 120 °C; ring lens, 10 V; and orifice 2, 5 V. These settings maximized the protonated water dimer $[(H_2O)_2 + H]^+$ with m/z 37, which implied that collision-induced decompositions that occur in the interface were minimized. To maximize sensitivity across a broad mass range of 10–1000 u, the radio frequency (RF) ion guide voltage was swept from 100 to 2500 V, with an initial hold time of 60% and a sweep time of 20% of the spectrum record time, during acquisition of each spectrum. The spectrum recording interval was 1.00 s, wait time 0.03 s, and data sampling interval 1 ns. The mass resolving power $(m/\Delta m)$ of the TOF was 6000 (full width at half maximum, FWHM) at 700 u. The m/z scale was calibrated using water and methanol clusters, and polyethylene glycol (PEG-600), ions from a methanol solution in a global calibration (calibration file acquired independently of sample file). This method of calibration in conjunction with scanning the ion guide resulted in an average mass accuracy of ±3 mmu across the mass range, which is equivalent to ±8 ppm at m/z 40 and ±1 ppm at m/z 500. This is less accurate than the manufacturer specified ±2 mmu and significantly less than what is achievable by using a static ion guide voltage and internal calibration (spectrum of calibrant acquired as part of sample file) [30]. Background spectra were acquired for all analyses and were subtracted from the spectra of the samples.

The DART ion source was operated using a flow of helium that was registered as 5.0 L min^{-1} by the MS software but was measured actually to be 5.77 L min^{-1} (number of measurements (n) = 5; relative standard error (RSE) = 1.01%). The actual flow rate was measured by using a Gilmont GF-8522-1606 rotameter that had been calibrated by the National Institute of Standards and Technology (NIST) as reporting a flow rate for helium of 20.4 L min^{-1} at the maximum scale reading. Measurements were made by connecting the rotameter to the ceramic outlet of the ion source using Tygon tubing.

The ceramic outlet of the ion source was positioned 10 mm from the pinhole orifice that leaks into the mass analyzer. The temperature of the helium exiting the ion source was measured at a distance of 1 mm from the ceramic outlet using a Control Company Traceable Dual-Channel Thermometer with a type-K beaded thermocouple probe. This digital thermometer has a sampling time of 0.8–1.0 s and an accuracy of ±0.75% or ±1 °C (whichever is greater).

All equipment to contact paper samples was cleaned using rinses of purified water, acetone, and dichloromethane (Pesticide Residue Analysis or comparable grades, Fisher Scientific) to remove plasticizers and other organic contaminants. Paper sheets were either cut into 6.4 mm diameter samples using a commercial hand-held paper hole punch, or microsamples were obtained by tweezing fiber bundles from the papers under a microscope. Samples were positioned at room temperature in the helium at a distance of 1 mm from the ceramic outlet of the ion source by using fine-point stainless steel tweezers.

Two types of experiments were conducted that involved heating the helium to higher temperatures. One involved equilibrating the helium at different temperatures that were set using the MS

Table 1
Furnish description of the 15 ASTM-ISR papers.

Number	First pulp type	Second pulp type	pH of stock[b]	pH-control chemical[c]	$CaCO_3$ (PCC) filler[c]	External sizing[c]	Internal sizing[c]
1	100% BNSWK	–	5.0	Alum	–	–	Rosin
2		–	8.1	Na_2CO_3	5%	–	–
3	100% SW-BCTMP	–	5.0	Alum	–	–	–
4		–	8.1	Na_2CO_3	5%	–	–
5[a]	100% COTTON	–	5.0	Alum	–	–	Rosin
6[a]		–	8.1	Na_2CO_3	5%	–	–
7	20% BNSWK	80% SGW	5.0	Alum	–	–	–
8			7.0	SMI Process	5%	–	–
9	20% BNSWK	80% HW-BCTMP	8.1	Na_2CO_3	–	–	–
10			8.1	Na_2CO_3	5%	–	–
11	50% BNSWK	50% BNHWK	8.1	Na_2CO_3	–	–	–
12			8.1	Na_2CO_3	5%	–	–
13	50% BNSWK	50% HW-BCTMP	8.1	Na_2CO_3	5%	–	–
14			5.0	Alum	–	–	Rosin
15	50% BNSWK	50% BNHWK	8.1	Na_2CO_3	5%	Penford Gum 270	AKD

[a] Samples 5 and 6 were produced by Crane and Co., Inc. at their Dalton, MA paper mill on their Fourdrinier "Pioneer" paper machine. All other papers were made on a 36-inch Fourdrinier paper machine at the Herty Foundation in Savannah, GA. In the table above, the letter designations have the following meanings: SW, softwood; HW, hardwood; BNSWK, bleached northern softwood kraft pulp; BNHWK, bleached northern hardwood kraft pulp; BCTMP, bleached chemithermomechanical pulp; SGW, stone groundwood pulp; SMI, Specialty Minerals, Inc.; AKD, alkyl ketene dimer sizing.

[b] pH is of the stock, not the paper, in which the stock is the watery pulp that contains all the additives prior to producing the paper on the papermaking machine.

[c] Alum (aluminum sulfate, $Al_2(SO_4)_3 \cdot 14H_2O$) was dry, iron-free (General Chemical Corp.); Na_2CO_3 (soda ash) was from FMC, Inc.; precipitated calcium carbonate (PCC) was from Specialty Minerals, Inc.; Penford Gum 270 was from Penford Products Co.; rosin was Neuphor 635 anionic dispersed sizing (Hercules, Inc.); and AKD was Hercon 70 reactive sizing (Hercules, Inc.).

software and then acquiring background and sample spectra: an equilibration time of 15–30 s was needed to obtain a stable temperature reading. A second involved ramping the temperature of the helium using the MS software: the software was set to a temperature of 20 °C, the helium was allowed to equilibrate (to an actual temperature of 55 °C), data acquisition was begun, background spectra were acquired, a sample was positioned in the helium, and then the software temperature setting was changed to 500 °C. When the software temperature reading reached 450 °C, data acquisition was halted. This procedure gave a 125 °C min^{-1} ($n = 7$, RSE = 2.5%) rate of change of temperature of the helium as measured at the outlet of the ion source ceramic. The MS software used in these experiments does not permit ramping of the temperature at operator-defined rates.

2.2. Reference papers

The sixteen reference papers analyzed include 15 ASTM-ISR printing and writing papers stored at the Library of Congress and Whatman #1 100% cotton cellulose filter paper.

2.2.1. Furnish descriptions

The furnish descriptions for each of the ASTM-ISR papers are given in Table 1, in which "furnish" refers to the aqueous suspension or "stock" of the fibrous materials and all additives that are being prepared for conversion into paper [4]. The ASTM-ISR papers were manufactured in 1995 at paper mills under controlled conditions and chemical specifications (Table 1). Papers made from cotton (ASTM-ISR papers #5 and #6) and bleached kraft wood pulps (ASTM-ISR papers #1, #2, #11, #12, and #15) may be considered "wood-free" because they are highly purified and primarily contain cellulose. Cotton pulps are used in currency paper, and bleached kraft pulps are used in fine writing papers. Paper #6 may be considered a close model of stable alkaline pre-1650 rag papers that contain natural carbonates but without gelatin sizing. Paper #5 more closely reflects rag papers from the late 1800s to 1900s that contain acidic alum-rosin sizing. Kraft papers #1 and #2, which reflect 20th century technologies, either are acidic and contain alum-rosin sizing or are alkaline and contain $CaCO_3$ as filler, respectively. Calcium carbonate fillers have been used since the early 1900s to provide an increase in paper opacity, brightness, and

Table 2
Characteristics of pulps used in the ASTM-ISR papers.

Furnish	Species	Fiber length (mm)[b]	α-Cellulose (%)[c]	Extractives (%)[d]	Kappa number[e]	Klason lignin (%)[f]
BNSWK	100% Softwood 70–80% Spruce 20–30% Jack pine 5–10% Balsam fir	2.75	84	0.050	0.81	≤0.1
BNHWK	96% Hardwood *Populus* sp. 4% Softwood Spruce and jack pine	0.97	93	0.18	0.77	≤0.1
SW-BCTMP	100% Softwood >95% Spruce <5% Jack pine	2.25	–	0.12	23	~3 to 4
HW-BCTMP (Millar Western Mill)[a]	100% Hardwood *Populus* sp.	0.98	–	0.13	23	~3 to 4
HW-BCTMP (Tembec Mill)[a]	100% Hardwood *Populus* sp.	0.90	–	0.15	23	~3 to 4
SGW	100% Softwood *Picea* sp.	–	–	–	–	–
Cotton	*Gossypium hirsutum*	27–29	–	–	–	–

[a] Papers that contained HW-BCTMP were made from equal mixtures of the two HW-BCTMP pulps.

[b] Weighted average. The 100% cotton paper was made from long-staple textile-grade cotton fiber [31].

[c] Determined at paper mill using TAPPI standard method T203 om-93 (current designation: T203 cm-99) [32]. This method can only be used for delignified pulps.

[d] Determined at paper mill using TAPPI T204 om-88 (current designation: T204 cm-07) [33].

[e] Determined at paper mill using TAPPI um-251 (current designation: T236 om-06) [34].

[f] Percent (%) klason lignin was calculated from (Kappa number × 0.13) [34] and (Kappa number × 0.17) [35].

bulk [3]. Other wood-free papers #11, #12, and #15 represent the finest modern (late 20th–21st century) printing and writing papers. In particular, paper #15 is a high-quality bleached kraft alkaline paper that contains a late 20th-century internal sizing agent, alkyl ketene dimer (AKD), and an external gum sizing (a hydroxyethyl ether derivative of cornstarch).

Several "wood-containing" papers contain either stone ground-wood (SGW) or bleached chemithermomechanical pulps (BCTMP). Papers #7 and #8 are similar to wood pulp papers from 1800s to 1900s: modern stone groundwood pulp is manufactured using essentially the same process that was developed in 1800s [3,4]. Although stone groundwood was used in 1800s and early 1900s for many types of papers, it is primarily used now in newsprint. The other wood-containing papers (ASTM-ISR papers #3, #4, #9, #10, #13, #14) were made using BCTMP, which is a late 20th-century high-yield wood pulp that is increasingly being used in coated papers and added to copy/offset/inkjet papers, as described more in Section 2.2.2.

2.2.2. Pulp characteristics

Some general characteristics of the pulps used in the papers are given in Table 2. The two kraft pulps, one softwood (spruce, pine, and fir) and one hardwood (aspen), were delignified using the alkaline sulfate kraft process followed by bleaching, which removes most of the hemicelluloses, extractives (lipophilic phytochemicals such as fatty acids and alcohols, triglycerides, waxes, terpenoids, lignans, steroids and sterols, stilbenes, and flavonoids [3,36–38]), and lignin. The softwood kraft (BNSWK) pulp contains a small percentage of extractives (0.05%) and lignin ($\leq$0.1%). The hardwood kraft (BNHWK) pulp contains four times as much extractives (0.18%) than the softwood pulp, although the amount of lignin in both pulps is comparable.

The bleached chemithermomechanical pulps (BCTMP) are mechanical pulps that are pretreated with steam and a hot solution of sodium hydroxide and/or sodium sulfite to soften the wood chips prior to defibering so that the pulp has longer fibers, higher strength, and lower fines as compared to stone groundwood pulp [3,4]. The pulp is bleached using hydrogen peroxide (totally chlorine free, or TCF, bleaching), which removes conjugation (chromophores) but not the lignin [39,40]. Consequently, the amount of lignin is significantly higher in the BCTMP than the kraft pulps (3–4%), but the amount of extractives is comparable to the hardwood kraft pulp (Table 2). The TAPPI (founded in 1915 as the Technical Association of the Pulp and Paper Industry) standard methods that were used to provide the analytical data in Table 2 [32–34] give no information regarding the identities of the extractives.

The stone groundwood (SGW) pulp is a softwood (spruce) mechanical pulp. There are no chemical treatments involved, so this pulp contains all the cellulose, hemicelluloses, extractives, and lignin that are contained in the original wood.

The final pulp is 100% cotton used in currency paper. The paper made from this pulp should be very pure and comparable in chemical composition to Whatman #1 filter paper, which is made from cotton linters.

3. Results and discussion

3.1. Temperature dependency of mass spectra

In developing the methodology for analysis of paper by using DART-MS, the temperature of the helium was found to significantly impact the information obtained. The first method that was evaluated involved setting the helium temperature to different static temperatures, and then inserting the paper into the helium stream.

This method was not useful, however, because it resulted in irreproducible flash vaporization of different substances depending on temperature. In contrast, the most thorough and repeatable analyses were obtained by ramping the temperature of the helium from ambient to a high temperature during data acquisition to obtain the temperature-dependent spectra of all the substances evolved. This is demonstrated in Fig. 1 for the analysis of a high-cellulose paper that contains late 20th-century alkyl ketene dimer (AKD) internal sizing. The total ion chromatogram (TIC) (Fig. 1a) shows that: (1) from time 0.6 to 1.3 min, a piece of organic-free aluminum was inserted into the helium stream to provide a "blank" spectrum of all species in the laboratory air that appear to arise from the turbulence of the gas as a result of simply inserting an object into the gas stream; (2) at time 1.8–2.6 min, a sample was positioned in the helium stream to reduce the intensity counts to ~25% of the air background; and (3) from time 2.6 to 7.2 min, the temperature of the helium was software-ramped from 20 to 500 °C. The scales in Fig. 1a show the relationship between ramp time and the actual (as opposed to software) temperature of the helium striking the sample up to approximately 350 °C. By the end of the analysis (when the software temperature reading reached 450 °C), charring was evident and the size of the 6.4-mm diameter sample had been reduced by ~200 μm.

The background-subtracted spectra in Fig. 1b–e show how different substances, which will be discussed in Sections 3.2–3.3, are detected at different temperatures. As the helium temperature rises to ~150 to 250 °C (Fig. 1b), intact polar organic compounds (~200 to 600 u) from sizing, extractives, and/or other semi- to nonvolatile organic substances are evolved. At temperatures of ~250 to 350 °C (Fig. 1c), low-mass thermolysis products (~40 to 200 u) from cellulose are clearly seen. At temperatures >350 °C (Fig. 1d), the low-mass cellulose-derived ions dominate. Although each temperature range provides different detailed information about the paper constituents, a composite "fingerprint" of both the paper substrate and other substances present can be obtained by software averaging all spectra across all temperatures (Fig. 1e). These "temperature averaged" mass spectra, which contain all the chemical information, are used for the DART mass spectral library.

### 3.2. Whatman #1 (cotton) and bleached kraft papers

The temperature-averaged spectrum shown in Fig. 1e of a high-cellulose kraft wood pulp paper that contains a modern sizing can be compared to spectra of cotton and other types of high-cellulose wood-pulp papers (Fig. 2). The background-subtracted, temperature-averaged spectrum of Whatman #1 filter paper (100% cotton cellulose) is shown in Fig. 2a. The low-mass series of peaks arises from the thermal decomposition of cellulose that primarily occurs at >250 °C. The thermolysis products are volatiles that arise from dehydration and thermolytic chain scission reactions [41]. Many products are of the same elemental formulae reported from Py-MS of cellulose, carbohydrates, and Whatman paper (Table 3) [20,41,42]. There are some, however, that have not been previously reported, and their structures are suggested here with basis in structure and formula searches of the NIST05 NIST/EPA/NIH Mass Spectral Library [43] and on-line chemical search engines (primarily ChemSpider [44] and ChemExper [45]). There are also products not observed in the DART-MS spectra that are seen in Py-MS spectra.

The structures in Table 3 and the differences between DART-MS and Py-MS spectra provide insight into the types of structures that seem to be preferentially detected by DART-MS. In particular, all the products shown in Table 3, and their structural isomers, are highly oxidized and highly stable, in many cases because of charge delocalization. Most noticeably, saturated products that contain alcohol functionalities that are observed in Py-MS spectra [20,41,42] are neither observed nor suggested here as structures because proto-
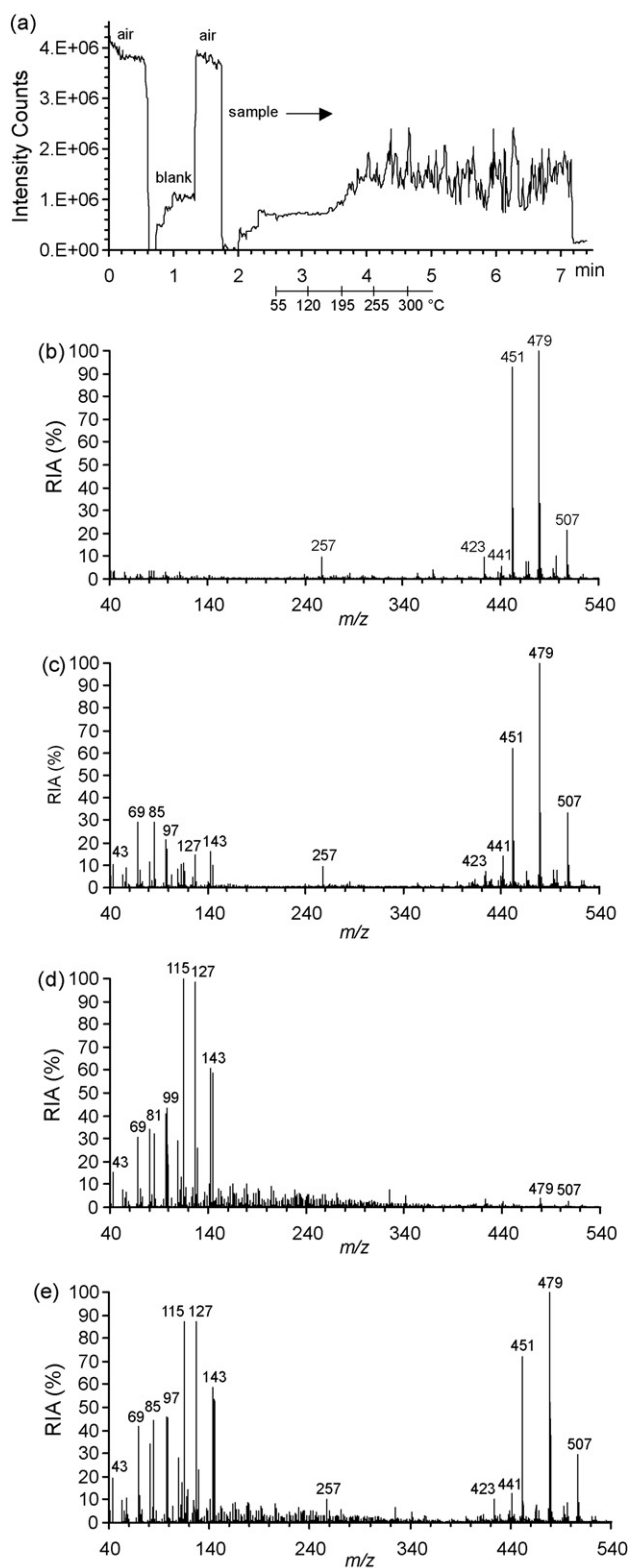
Fig. 1. Data for a high-cellulose 50/50 bleached softwood/hardwood kraft paper that contains alkyl ketene dimer (AKD) internal sizing (ASTM-ISR paper #15): (a) total ion chromatogram (TIC) with temperature scale that shows the actual temperature of the helium striking the sample; (b) mass spectrum of compounds evolving at ∼150 to 250 °C; (c) mass spectrum of compounds evolving at ∼250 to 350 °C; (d) mass spectrum of compounds evolving at >350 °C; and (e) mass spectrum from software averaging the spectra acquired across all temperatures.
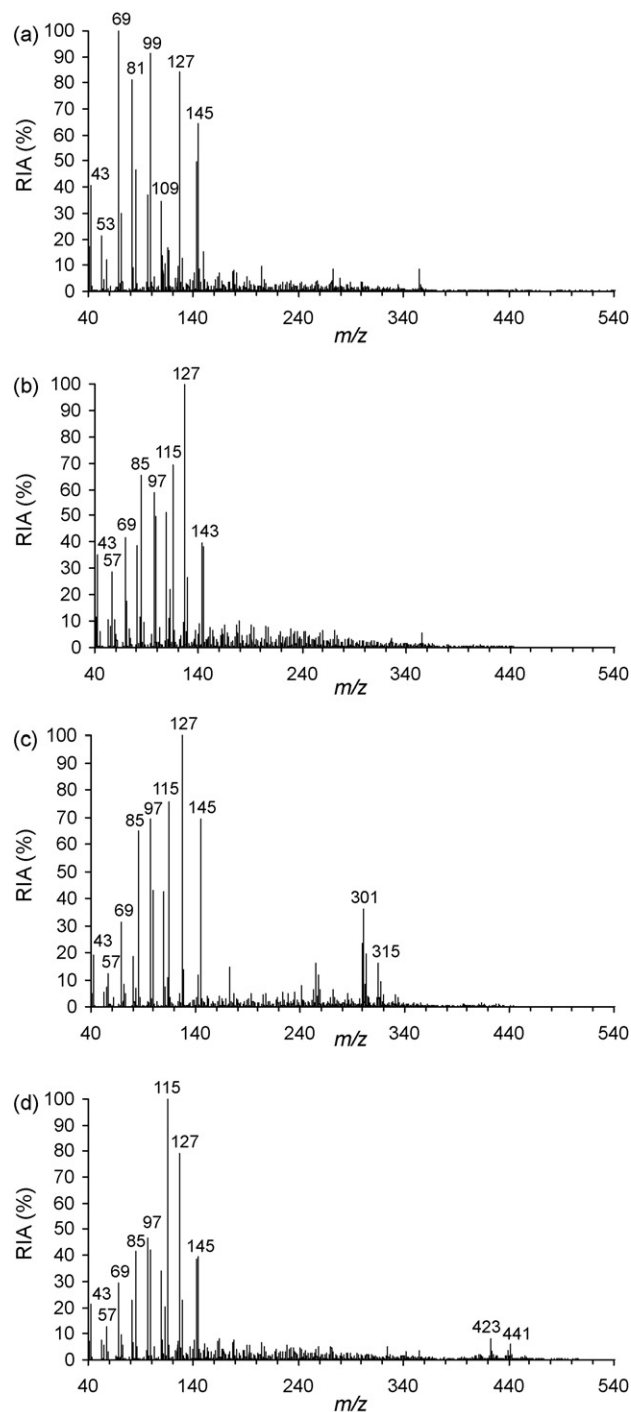
Fig. 2. Spectra (after subtracting the blank and software averaging across all temperatures) of high-cellulose papers made from: (a) 100% cotton (Whatman #1); (b) 100% bleached northern softwood kraft (BNSWK) pulp (ASTM-ISR paper #2); (c) 100% BNSWK pulp with alum-rosin sizing (ASTM-ISR paper #1); and (d) 50% BNSWK/50% BNHWK pulp (ASTM-ISR paper #12).

nation of saturated alcohols in the DART ionization process would result in loss of water, generating in many cases unstable carbocations in analogy to classic proton-transfer chemical ionization.

The structures represented by ions with m/z values 43–117 suggest that ions with m/z values 127–145 may also be similarly oxidized. In particular, ions with m/z 127 and m/z 145 can have different isomeric structures including the $(M+H)^+$ ions of levoglusenone (m/z 127) and 1,4:3,6-dianhydro-α-ᴅ-glucopyranose (m/z 145) [19,41]. However, more oxidized structures are also fea-

Table 3
Ions derived from the high-temperature thermolysis of cellulose that are present in positive ion DART-MS spectra of paper.
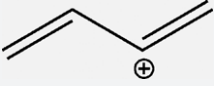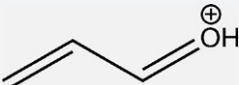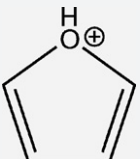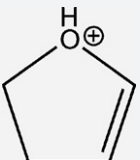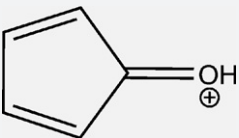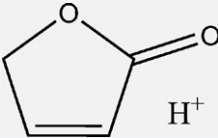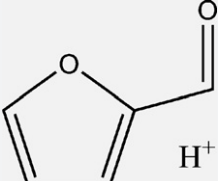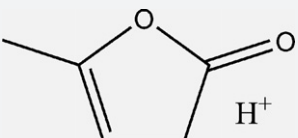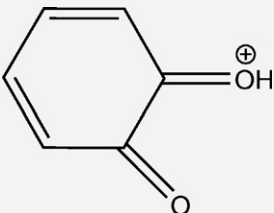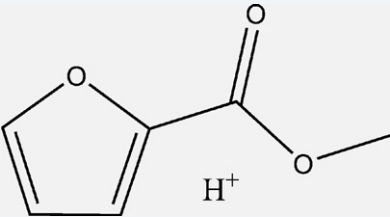
m/z (theoretical)	Formula	Suggested ion structure	Suggested protonated molecule or fragment[a]
43.018	$C_2H_3O^+$	$H_3C-C{\equiv}O^{\oplus}$	Acylium ion[b]
		$H_2C{=}C{=}OH^{\oplus}$	Ketene[b]
53.039	$C_4H_5^+$		1,3-Butadiene cation[b]
57.034	$C_3H_5O^+$		2-Propenal
69.034	$C_4H_5O^+$		Furan
71.050	$C_4H_7O^+$		2,3-Dihydrofuran
81.034	$C_5H_5O^+$		Cyclopenta-2,4-dien-1-one[b]
85.029	$C_4H_5O_2^+$		2-Furanone
97.029	$C_5H_5O_2^+$		2-Furaldehyde [fufural]
99.045	$C_5H_7O_2^+$		5-Methyl-2-furanone
109.029	$C_6H_5O_2^+$		1,2-Benzoquinone[b]

Table 3 (*Continued*)
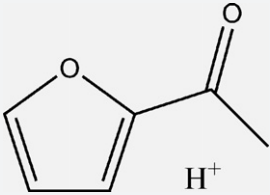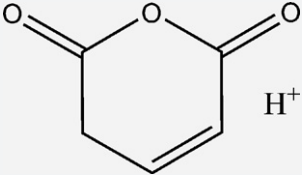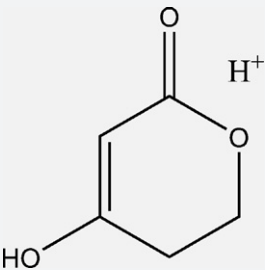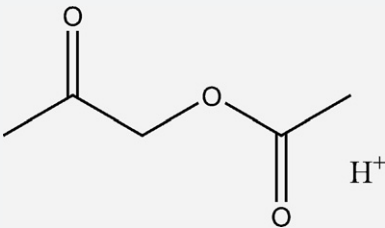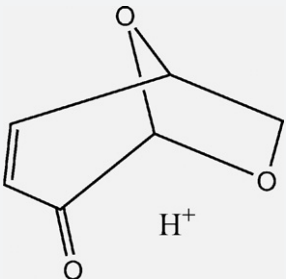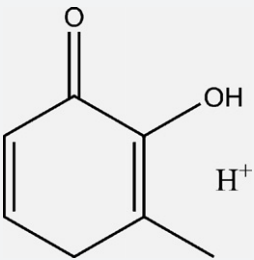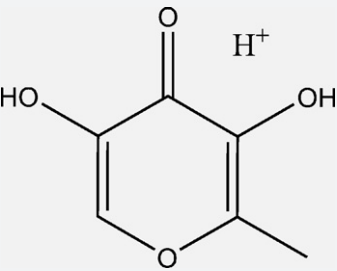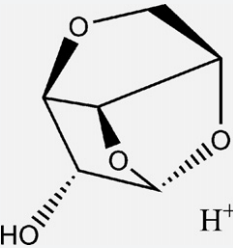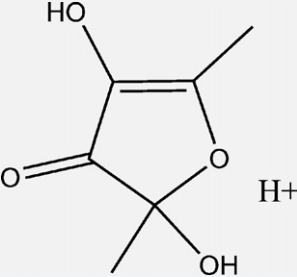
m/z (theoretical)	Formula	Suggested ion structure	Suggested protonated molecule or fragment[a]
111.045	$C_6H_7O_2^+$		2-Acetylfuran
113.024	$C_5H_5O_3^+$		2H-pyran-2,6(3H)-dione
115.040	$C_5H_7O_3^+$		4-Hydroxy-5,6-dihydro-(2H)-pyran-2-one
117.055	$C_5H_9O_3^+$		1-Acetoxy-2-propanone
127.040	$C_6H_7O_3^+$		6,8-Dioxabicyclo[3.2.1]oct-2-en-4-one [levoglusenone]
			3-Hydroxy-2-methyl-(4H)-pyran-4-one

Table 3 (*Continued*)

m/z (theoretical)	Formula	Suggested ion structure	Suggested protonated molecule or fragment[a]
			2-Furoic acid methyl ester
143.034	$C_6H_7O_4^+$		3,5-Dihydroxy-2-methyl-pyran-4-one
145.050	$C_6H_9O_4^+$		1,4:3,6-Dianhydro-α-D-glucopyranose
			2,4-Dihydroxy-2,5-dimethyl-furan-3-one[b]

[a] Structures suggested from data in ref. 20, 41, and 42 except as noted. Although ions with *m/z* 113 could be (M + H)[+] ions of 2-furoic acid, this possibility was eliminated because its (M − H)[−] anions were not detected by using negative ion DART-MS. Another possible structure for ions with *m/z* 115 would be a methylhydroxy furanone. This possibility was eliminated because the protonated hydroxyl group would have been lost as H_2O in analogy to proton-transfer chemical ionization (see discussion in text).

[b] Structures suggested here.

sible and previously reported for these two products that may be the species detected by DART-MS (Table 3).

The mass spectrum of a bleached softwood kraft paper (ASTM-ISR paper #2) is virtually identical to the spectrum of Whatman filter paper in terms of products present (Fig. 2b). The high level of purity of this paper as revealed by the spectrum is in accord with data in Table 2 that show that this pulp contains a high level of cellulose and minimal extractives or lignin.

When alum-rosin sizing is added to the bleached softwood kraft paper (ASTM-ISR paper #1), the mass spectrum immediately reveals the presence of the rosin (Fig. 2c). The resin acid protonated molecules, which begin to appear at ∼150 °C and reveal the presence of the rosin sizing, are $(C_{20}H_{28}O_2 + H)^+$ from dehydroabietic acid with *m/z* 301.217 $(C_{20}H_{30}O_2 + H)^+$ from primarily abietic acid with *m/z* 303.232, and $(C_{20}H_{26}O_3 + H)^+$ from 7-oxodehydroabietic acid with *m/z* 315.196 [35]. The vapor pressures (VPs at 298 K) of the rosin acids are estimated to be ∼10[−6] to 10^{−7} Pa [44], so these types

of relatively nonvolatile polar organic compounds may be observed directly by using DART-MS at lower temperatures without the need for derivatization and gas chromatography.

When bleached hardwood kraft pulp is mixed with the bleached softwood kraft pulp, the spectrum of the resultant paper reveals the appearance of two new higher mass ions with *m/z* 423 and *m/z* 441 that primarily begin to appear at ∼250 °C (Fig. 2d). Peaks representing these ions also appear in spectra in Fig. 1 of the 50/50 bleached softwood/hardwood kraft paper that contains AKD sizing. Hardwoods such as *Populus* sp. (aspen) contain higher concentrations of steryl ester extractives than softwoods; oxidized sterols and triterpene alcohol products are formed during kraft pulping and bleaching of aspen [35,37]; and data in Table 2 indicate the presence of residual extractives in papers made from the bleached hardwood kraft pulp. These data suggest that these two ions arise from oxidation and/or dehydration of α-sitosterol and α-amyrin, respectively, perhaps as proposed in Scheme 1. α-Sitosterol could
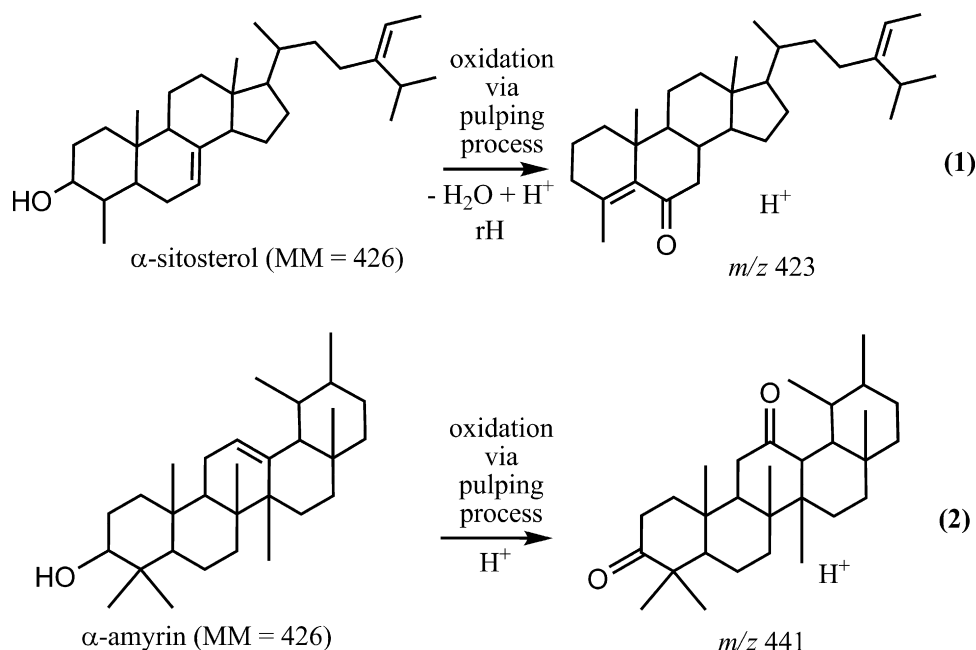
Scheme 1. Suggested origins of ions with *m/z* 423 (Eq. (1)) and *m/z* 441 (Eq. (2)) in spectra of bleached hardwood kraft papers (ASTM-ISR papers #11, #12, and #15). See spectra in Figs. 1 and 2d.

be oxidized during kraft pulping and bleaching to give an oxo structure, which would then lose water either before or after protonation by the DART ionization process to give the ion with *m/z* 423 (Eq. (1), Scheme 1). α-Amyrin could be oxidized during kraft pulping and bleaching to give another oxo structure, which would then be protonated by the DART ionization process to produce the ion with *m/z* 441 (Eq. (2), Scheme 1). The VPs of α-sitosterol and α-amyrin are estimated to be ∼10⁻⁹ Pa [44], so DART-MS can detect some highly involatile polar organic compounds at higher temperatures without thermal fragmentation.

Another notable difference between spectra of softwood and hardwood kraft papers in Fig. 2 is the different intensities of the peak representing ions with *m/z* 115, $(C_5H_6O_3 + H)^+$. This ion is a thermolysis marker for the hemicellulose xylan, which is significantly more predominant in hardwoods than softwoods [46,47]. This peak is of low relative abundance in the spectrum of Whatman #1 (Fig. 2a), is ∼70% to 80% abundant in the spectrum of the softwood kraft paper (Fig. 2b and c), but is the most abundant peak, particularly in relation to the other carbohydrate-derived peaks, in the spectrum of the hardwood kraft paper (Fig. 2d). These data show that the bleached hardwood kraft paper may be differentiated from the bleached softwood kraft paper by the presence of ions from residual hardwood extractives and xylan.

A comparison of the spectrum in Fig. 1e to the spectrum in Fig. 2d shows how the presence of the modern alkyl ketene dimer (AKD) sizing agent is revealed. The starting material for the AKD was a 60/40 mixture of palmitic and stearic acids that were converted into acid chlorides, which then underwent intermolecular lactone ring condensations to give the final alkyl ketene dimers. The peak in Fig. 1e that represents ions with *m/z* 257 arises from residual palmitic acid $[C_{16}H_{32}O_2 + H]^+$. The three intense higher mass peaks in Fig. 1e are from protonation of the ketones formed by hydrolysis of AKD: hentriacontan-16-one $(C_{31}H_{62}O + H)^+$ with *m/z* 451.488, tritriacontan-16-one $(C_{33}H_{66}O + H)^+$ with *m/z* 479.519, and pentatriacontan-18-one $(C_{35}H_{70}O + H)^+$ with *m/z* 507.550 [16]. All these intact molecules begin to be evolved at ∼150 °C even though the estimated VP of pentatriacontan-18-one (∼10⁻⁹ Pa) is six orders of magnitude smaller than the VP of palmitic acid

(∼10⁻³ Pa) [44]. These data indicate that the temperatures at which intact molecules are vaporized from paper by using DART ionization are related to other factors and not simply their VPs.

3.3. Mechanical pulp papers

Spectra of the relatively pure papers discussed above primarily reveal products from the volatilization of sizings and two residual hardwood phytosteroids, plus products from the higher temperature thermolysis of cellulose and xylan. In contrast, spectra of mechanical pulp papers are significantly more complex and reveal products from lignin and phytochemicals not observed from the high-cellulose papers (Fig. 3 and Table 4).

3.3.1. Hardwood bleached chemithermomechanical pulp (HW-BCTMP)

Mixing a hardwood (aspen) BCTMP with the softwood kraft pulp results in paper whose spectra shows products from lignin-related structures (Fig. 3a; column five of Table 4). The spectra are somewhat visually similar to spectra of aspen wood and lignin obtained by using Py-molecular-beam sampling MS [48]; spectra of beech wood obtained by using temperature-programmed Py-field ionization MS [49]; spectra of cottonwood lignin obtained by using temperature-programmed in-source Py-MS [50]; and spectra of *Aesculus turbinata* lignin obtained by using in-source Py-MS [51]. However, upon close inspection, there are more differences than similarities between the DART-MS spectra and those obtained by using Py-MS. The two lowest mass resonance stabilized monomeric benzofuran products in the DART-MS spectra (*m/z* 131 and *m/z* 161) have no apparent analogs in Py-MS spectra: Benzofurans can be formed from oxidation of phenylcoumaran lignin structures [52]. Peaks that represent molecular ions of coniferyl and sinapyl alcohols (*m/z* 180 and *m/z* 210, respectively) are seen in Py-MS spectra, but DART-MS spectra instead reveal peaks from the resonance stabilized allylic carbenium ions (*m/z* 163 and *m/z* 193, respectively) that arise by loss of water from the (M + H)⁺ ions of the two alcohols [50]. The oxidized forms of the alcohols, coniferaldehyde and sinapaldehyde, respectively, are seen in abundance by DART-MS

Table 4

Non-carbohydrate ions present in DART-MS spectra of papers that contain hardwood bleached chemithermomechanical pulp (HW-BCTMP) (ASTM-ISR papers #9, #10, #13, and #14), 100% softwood bleached chemithermomechanical pulp (SW-BCTMP) (ASTM-ISR papers #3 and #4), and stone groundwood (SGW) pulp (ASTM-ISR papers #7 and #8). See Fig. 3 for spectra.
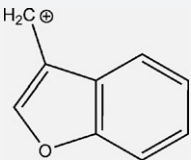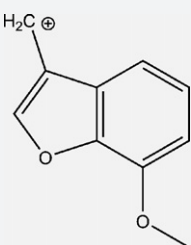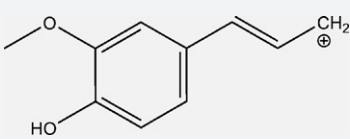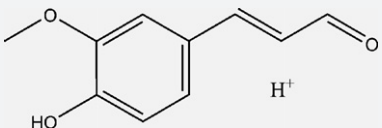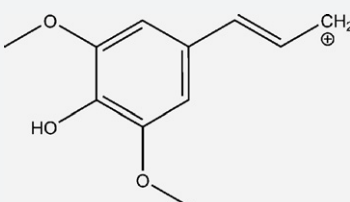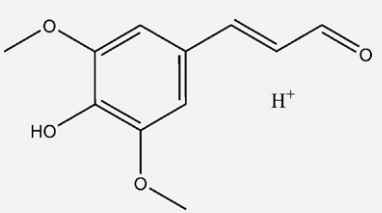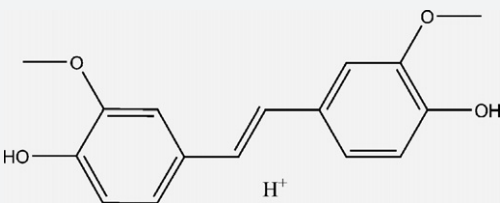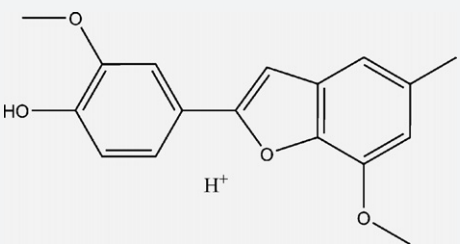
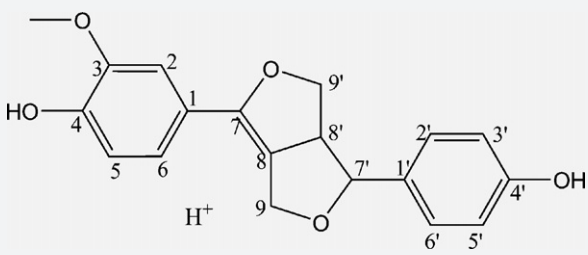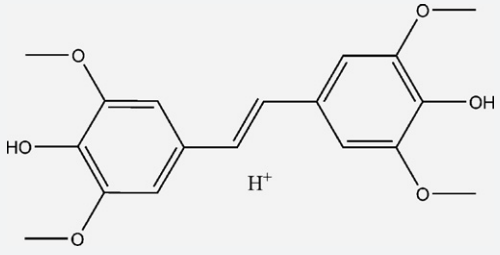| m/z (theoretical)	Formula	Suggested ion structure or fragment[a]	Suggested protonated molecule[a]	HW-BCTMP (%)[c]	SW-BCTMP (%)[c]	SGW (%)[c]
Lignin-derived ions						
131.050	$C_9H_7O^+$		3-Methyl-benzofuran[b]	61	97	100
161.060	$C_{10}H_9O_2^+$		7-Methoxy-3-methyl-benzofuran[b]	81	31	17
163.076	$C_{10}H_{11}O_2^+$		2-Methoxy-4-[prop-1-enyl] phenol	39	75	52
179.071	$C_{10}H_{11}O_3^+$		Coniferaldehyde[b]	52	100	77
193.086	$C_{11}H_{13}O_3^+$		2,6-Dimethoxy-4-[prop-1-enyl] phenol	67	30	12
209.081	$C_{11}H_{13}O_4^+$		Sinapaldehyde[b]	100	28	–
273.113	$C_{16}H_{17}O_4^+$		4,4′-Dihydroxy-3,3′-dimethoxystilbene (G-G dimer)	13	39	33
285.113	$C_{17}H_{17}O_4^+$		G-G phenylcoumarone dimer[b]	–	18	–

Table 4 (*Continued*)
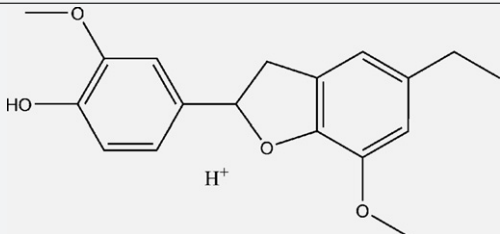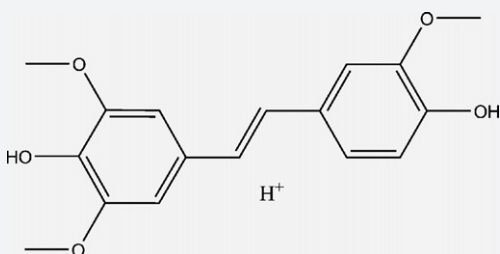
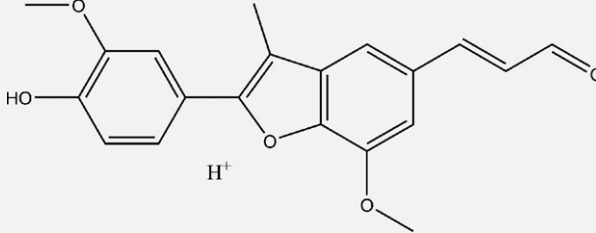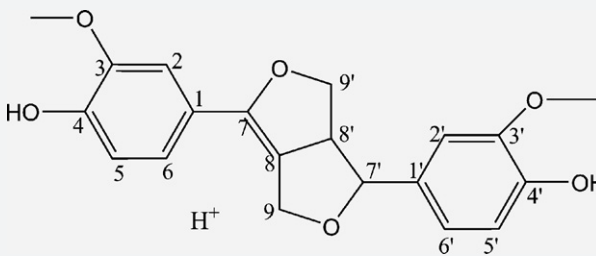| m/z (theoretical)	Formula	Suggested ion structure or fragment[a]	Suggested protonated molecule[a]	HW-BCTMP (%)[c]	SW-BCTMP (%)[c]	SGW (%)[c]
301.144	$C_{18}H_{21}O_4^+$		G-G phenylcoumaran dimer	–	29	–
303.123	$C_{17}H_{19}O_5^+$		4,4′-Dihydroxy-3,3′,5-trimethoxystilbene (G-S dimer)	14	–	–
327.123	$C_{19}H_{19}O_5^+$		3′-Demethoxy-7-dehydropinoresinol[b] (C-G dimer)	–	38	33
333.134	$C_{18}H_{21}O_6^+$		4,4′-Dihydroxy-3,3′,5,5′-tetramethoxystilbene (S-S dimer)	20	–	–
339.123	$C_{20}H_{19}O_5^+$		G-G phenylcoumarone dimer[b]	–	21	18
357.134	$C_{20}H_{21}O_6^+$		7-Dehydropinoresinol[b] (G-G dimer)	19	12	13

Table 4 (*Continued*)
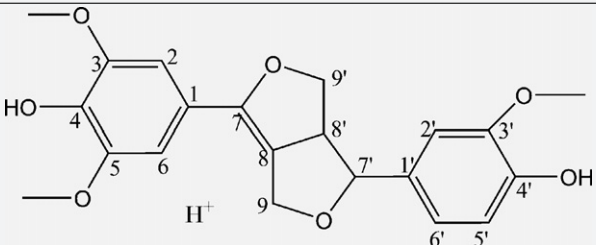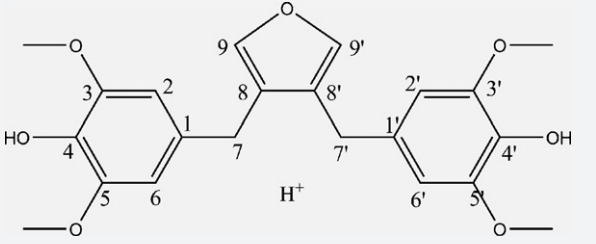
m/z (theoretical)	Formula	Suggested ion structure or fragment[a]	Suggested protonated molecule[a]	HW-BCTMP (%)[c]	SW-BCTMP (%)[c]	SGW (%)[c]
387.144	$C_{21}H_{23}O_7^+$		7-Dehydromedioresinol[b] (G-S dimer)	20	–	–
401.160	$C_{22}H_{25}O_7^+$		5,5′-Dimethoxy-8,8′-didehydro-3,4-divanillyltetrahydrofuran[b] (S-S dimer)	21	–	–
417.155	$C_{22}H_{25}O_8^+$		7-Dehydrosyringaresinol[b] (S-S dimer)	9	–	–
Extractives						
227.107	$C_{15}H_{15}O_2^+$		Pinosylvin methyl ether[b]	–	–	30
241.123	$C_{16}H_{17}O_2^+$		Pinosylvin dimethyl ether[b]	–	–	27
257.248	$C_{16}H_{33}O_2^+$		Hexadecanoic acid	–	–	52

Table 4 (*Continued*)

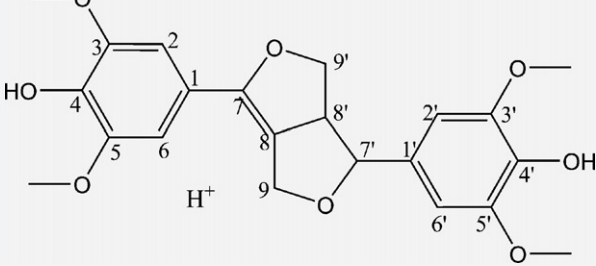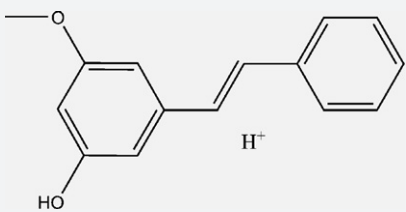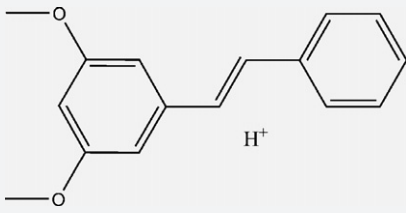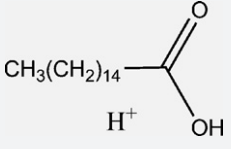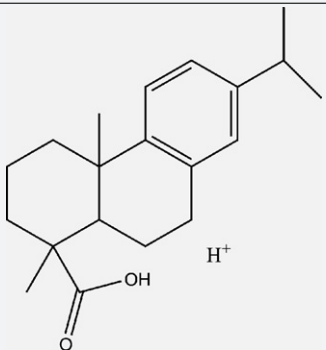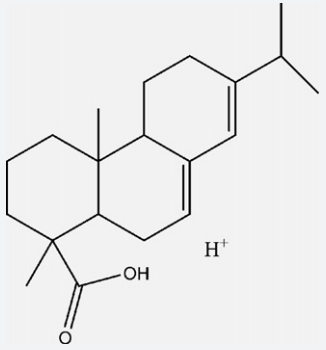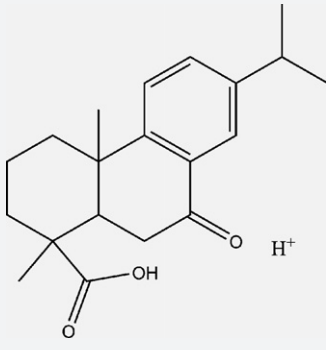| m/z (theoretical)	Formula	Suggested ion structure or fragment[a]	Suggested protonated molecule[a]	HW-BCTMP (%)[c]	SW-BCTMP (%)[c]	SGW (%)[c]
301.217	$C_{20}H_{29}O_2^+$		Dehydroabietic acid	–	–	60
303.232	$C_{20}H_{31}O_2^+$		Abietic acid (primary isomer)	–	–	66
315.196	$C_{20}H_{27}O_3^+$		7-Oxodehy droabietic acid	–	–	37
397.383	$C_{29}H_{49}^+$		Stigmastan-3,5-diene	–	–	10
411.363	$C_{29}H_{47}O^+$		Stigmasta-3,5-diene-7-one	–	–	17

Table 4 (Continued)

m/z (theoretical)	Formula	Suggested ion structure or fragment[a]	Suggested protonated molecule[a]	HW-BCTMP (%)[c]	SW-BCTMP (%)[c]	SGW (%)[c]
413.378	$C_{29}H_{49}O^+$		Stigmast-4-en-3-one (sitostenone)	–	–	5
429.373	$C_{29}H_{49}O_2{}^+$		Stigmastane-3,6-dione	–	–	9

[a] Structures suggested from data in Refs. [48–55] except as noted. Lignin phenylpropanoid unit designations are: C (p-hydroxyphenyl or coumaryl), G (guaiacyl), and S (syringyl).

[b] Structures suggested here.

[c] Percent relative ion abundances are ±15% (RSE).

(m/z 179 and m/z 209, respectively) but not observed by Py-MS. The estimated VPs of coniferaldehyde ($\sim 10^{-3}$ Pa) and sinapaldehyde ($\sim 10^{-4}$ Pa) [44] suggest that they should have been observed in the 150–250 °C temperature range, but all the monomeric lignin species (m/z 131–209) were instead primarily evolved at temperatures >250 °C. This suggests that they were not formed from volatilization by DART-MS but instead from thermolysis of lignin.

Some dimeric lignin structures are the same either by DART-MS or Py-MS, and others are different. The protonated stilbene structures seen by using DART-MS (m/z values 273, 303.1, and 333) have exact molecular ion counterparts by Py-MS. The stilbene analog that contains two guaiacyl groups (G-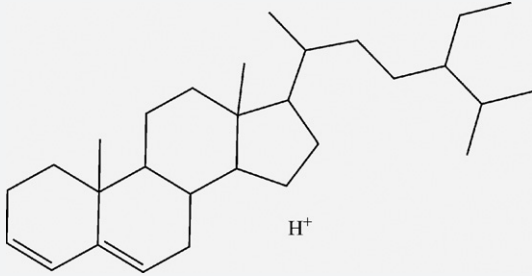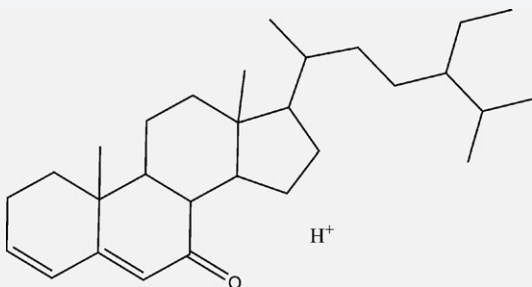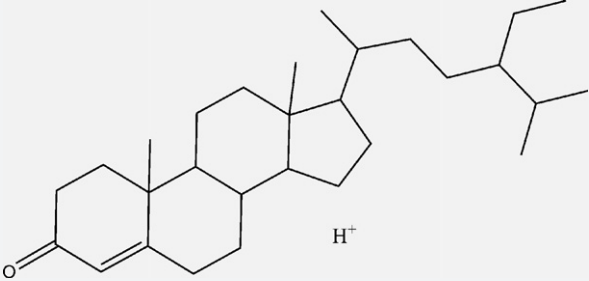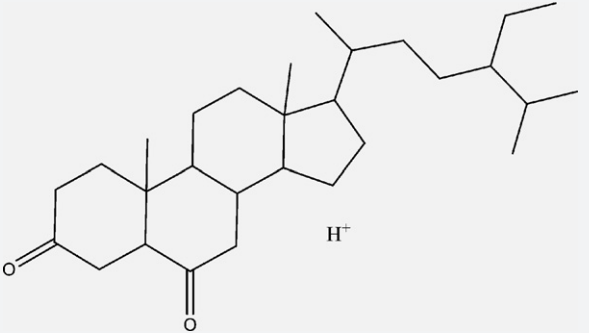G analog) with an estimated VP $\sim 10^{-6}$ [44] appears at ~ 150 °C, the analog that contains a guaiacyl and syringyl group (G-S analog) appears at ~ 250 °C, and the S-S analog appears at ~ 350 °C. These data suggest that the stilbenes may be volatilized as intact molecules, not primarily derived from thermolysis of the lignin. Confirmation of this would require extraction and analysis of both the paper extract and the extracted paper.

A series of three protonated ions with m/z values of 357, 387, and 417 are observed by using DART-MS that are oxidized versions of three molecular ions with m/z values 358, 388, and 418, respectively, that are instead observed by using Py-MS. These species are evolved primarily at >350 °C. Reasonable structures for each of the ions, with basis in previous hypotheses [49], are 7-dehydropinoresinol (m/z 357), 7-dehydromedioresinol (m/z 387), and 7-dehydrosyringaresinol (m/z 417), respectively (Table 4). Resinol-type lignin structures are very stable and expected to be observed from thermolysis of lignin at temperatures of ~ 325 to 400 °C [49].

There is one more ion of relevance with m/z 401. Its molecular ion counterpart with m/z 400 may be seen clearly in in-source Py-MS spectra obtained from wood of Calluna vulgaris and Aesculus turbinata [51,53] and from an organosolv lignin [54]. The structure suggested in Table 4 for this ion is that of an oxidized dimethoxy analog of 3,4-divanillyltetrahydrofuran (shonanin), which is a natural lignan whose syringyl analogs have been found in emissions from the combustion of both hardwoods and softwoods [55]. Its evolution at a temperature of ~ 250 °C may indicate that it is evolved as an intact molecule, not from thermolysis of lignin.

3.3.2. Softwood bleached chemithermomechanical pulp (SW-BCTMP)

The DART-MS spectra of softwood BCTMP papers (Fig. 3b) have features that distinguish them from hardwood BCTMP papers. Although the monomeric ions with m/z values of 131–209 arise from both types of paper, they are found in different relative abundances (compare columns five and six of Table 4). The relative abundances reflect the coumaryl (C) vs. G vs. S content of the lignin in which G-lignin is most abundant in softwood and S-lignin is most abundant in hardwood. Products from S-lignin units (m/z values 161, 193, and 209) dominate the spectrum of the hardwood paper (Fig. 3a) but products from G-lignin units (m/z values 131, 163, and 179) dominate the spectrum of the softwood paper.

Relative abundances of some of the dimer products also distinguish the papers. The only member of the stilbene series of ions that is detected from the softwood papers is the G-G dimer with m/z 273: the higher-mass dimers from the hardwood papers contain S-units. The only member of the resinol series of ions that is detected from the softwood papers is the G-G dimer with m/z 357: the higher-mass dimers from the hardwood papers contain S-units. The dimethoxy analog of 3,4-divanillyltetrahydrofuran (m/z 401) is not detected from the softwood papers because it is a S-S dimer.

There is one more feature in spectra of the softwood papers that differentiate them from the hardwood papers: the occurrence of four lignin product ions that are unique to the softwood papers. These include three G-G dimer products (with m/z 285, 301.1, and 339) that, with basis in previous hypotheses [49], are suggested to be phenylcoumarones (m/z 285 and m/z 339) and a phenylcoumaran (m/z 301.1) from lignin β-5 linkages abundant
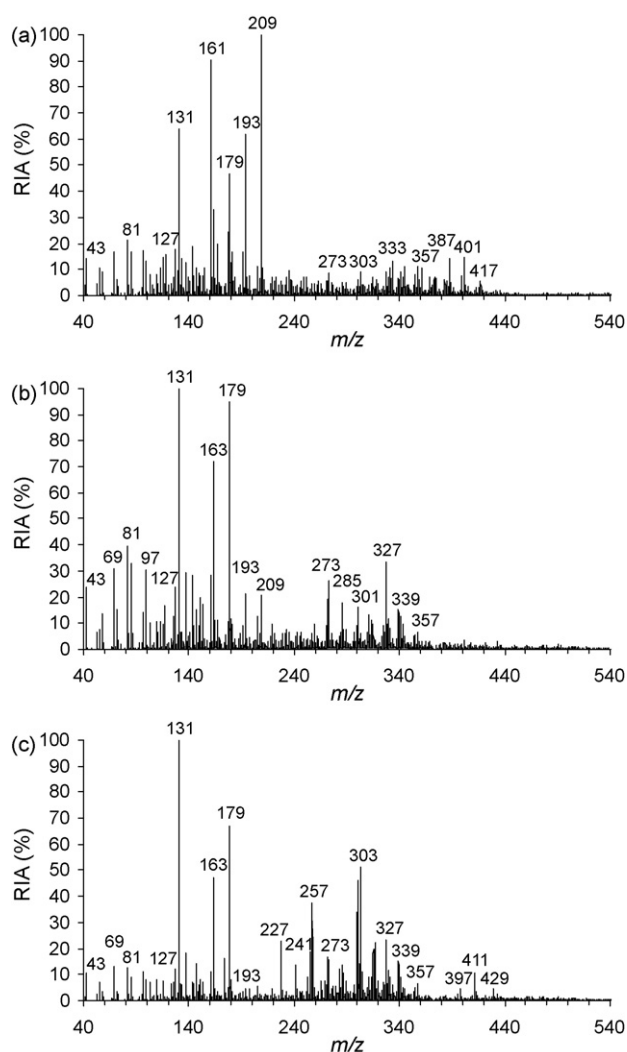
Fig. 3. Spectra of papers made from mechanical pulps: (a) 50% BNSWK/50% hardwood bleached chemithermomechanical pulp (HW-BCTMP) (ASTM-ISR paper #13); (b) 100% softwood BCTMP (SW-BCTMP) (ASTM-ISR paper #4); and (c) 20% BNSWK/80% stone groundwood (SGW) pulp (ASTM-ISR paper #8).

in softwood, and a demethoxy coumaryl-containing (C-G) dimer analog of the resinol series of ions (m/z 327).

As for hardwood papers, DART-MS spectra of softwood BCTMP papers also reveal lignin units that are more highly oxidized. However, Py-GC–MS spectra of *Picea* wood, thermomechanical pulp (TMP) made from the wood, and paper made from the TMP reveal no changes in the oxidation states of the products because of either the pulping or papermaking process [25]. Further, Py-GC–MS spectra of *Picea* wood and chemithermomechanical pulp (CTMP) made from the wood show a decrease in some of the more oxidized products after the CTMP process (less coniferaldehyde and more *trans*-coniferyl alcohol) [46]. Other studies show that hydrogen peroxide bleaching has little impact on the overall structure of TMP lignin other than to primarily eliminate coniferaldehyde end groups [39]. Hydrogen peroxide bleaching is also expected to remove conjugated double bonds, not generate them [46]. These data suggest that the detection of more highly oxidized (unsaturated) species by DART-MS is not a result of the pulping/bleaching process but is related to the DART ionization process itself.

3.3.3. Stone groundwood (SGW) pulp

Spectra of stone groundwood (SGW) pulp papers (Fig. 3c), which are made from unprocessed softwood chips, show some of the

same G-lignin (primarily from thermolysis) products as in spectra of papers made from softwood BCTMP but in different abundances. The monomeric G-lignin ions with m/z values of 131, 163, and 179 are present in high abundance, but S-lignin products with m/z values of 161, 193, and 209 are either significantly reduced or not detected (see column seven in Table 4). The only lignin dimers that are detected are the G-G stilbene product (m/z 273), the demethoxydehydropinoresinol C-G dimer (m/z 327), the G-G phenylcoumarone dimer (m/z 339), and the dehydropinoresinol G-G dimer (m/z 357). It is notable that the phenylcoumarone and phenylcoumaran G-G dimers seen in papers made from softwood BCTMP (m/z 285 and m/z 301.1, respectively) are not detected in spectra of papers made from softwood SGW pulp. This suggests that these two structures may be formed during the BCTMP process.

The most significant distinguishing feature of spectra of papers made from SGW pulp, however, is an extensive set of softwood extractives that are volatilized primarily at ∼150 °C (Table 4) [35–37,55]. The ten extractives include two pinosylvin methyl ethers (m/z 227 and m/z 241); hexadecanoic acid (m/z 257); three resin acids (m/z values of 301.2, 303.2, and 315); and four products derived from β-sitosterol (m/z values of 397, 411, 413, and 429). The $(M+H)^+$ ions of stigmastan-3,5-diene (m/z 397) most likely arise from loss of water from the $(M+H)^+$ ions of β-sitosterol in the DART ionization process because β-sitosterol is a highly abundant phytosterol found in extractives but not observed in the mass spectra. The three oxo phytosteroids (m/z values of 411, 413, and 429) are derived from the oxidation of β-sitosterol. Eight of the extractives are observed at ∼150 °C and have estimated VPs that range from ∼10^{-3} to 10^{-8} Pa. The two stigmasta 3,5-dienes (m/z 397 and m/z 411) are primarily observed at ∼250 °C and have estimated VPs of ∼10^{-7} [44].

3.4. Pitch extractives as contaminants in 100% cotton papers

Spectra of SGW pulp papers (Fig. 3c) show peaks from phytosteroids with m/z values 397, 411, 413, and 429 that also appear in spectra of currency-type papers made from 100% cotton pulp (ASTM-ISR papers #5 and #6) (Fig. 4). These data indicate that the cotton pulp was most likely contaminated by pitch. Strongly lipophilic compounds such as phytosteroids that survive pulping and/or bleaching processes are present as colloids that may be accumulated as pitch on papermaking machinery and found in recirculating water used in paper mills. Pitch colloids are generally associated with suspended solids and may be deposited in the final paper product [37].

3.5. Repeatability and sensitivity

DART-MS spectra need to be reproducible and repeatable for use in paper and other research. The 100% cotton paper that contains
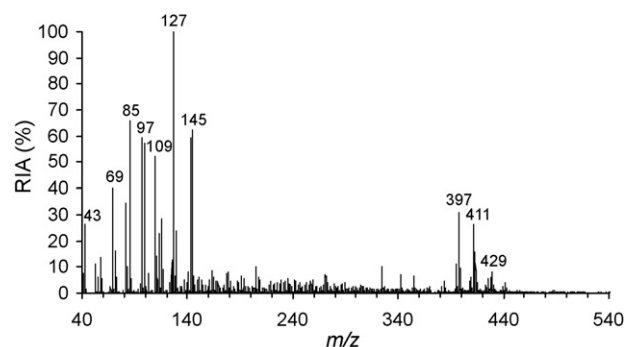
Fig. 4. Spectrum of paper made from 100% cotton at a paper mill (ASTM-ISR paper #6).
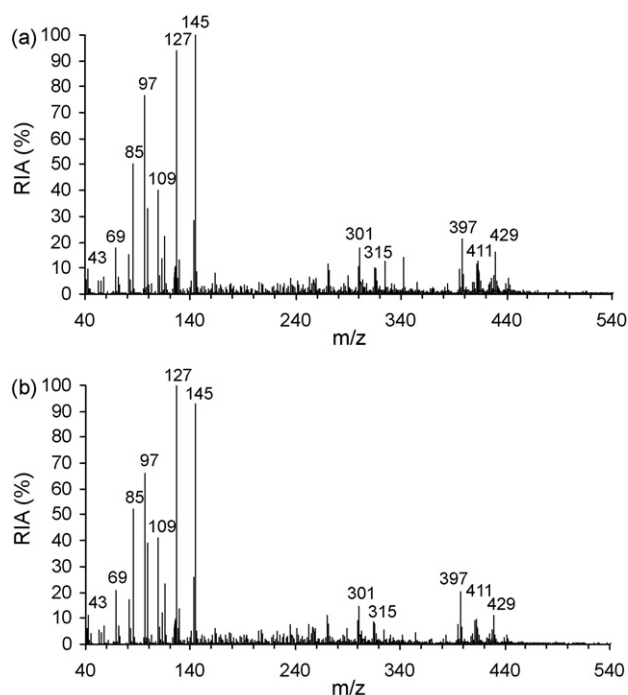
Fig. 5. Spectra from analyses of 100% cotton paper that contains alum-rosin sizing and pitch contaminants (ASTM-ISR paper #5) on two separate occasions (a and b).

Fig. 6. Spectra of 50% BNSWK/50%BNHWK paper that has AKD sizing (ASTM-ISR paper #15) obtained by using: (a) a 6.4-mm diameter piece of paper; and (b) an ~10-μg fiber bundle tweezed from the surface. The 10-μg fiber bundle is approximately the size of the period at the end of this sentence.

alum-rosin sizing and phytosteroid pitch contaminants (ASTM-ISR paper #5) was analyzed on two separate occasions. The resulting mass spectra (Fig. 5) demonstrate the repeatability of the analysis. The distinguishing ions with m/z values of 301, 315, 397, 411, and 429 have almost identical relative ion abundances (±15% RSE). An improvement in sample placement technique is expected to improve the repeatability, which is important for effective mass spectral database searches.

Another issue in reproducibility is the possible impact of inorganic salts on ion formation, particularly on products from thermolysis. In Py-MS, the presence, quantity, and identity of inorganic salts negatively impact pyrolytic behavior and spectral reproducibility [17]. This contrasts with results here in which papers that are made from the same pulp but differ in their inorganic components (Table 1) give virtually identical DART mass spectra that only differ if an organic component differs.

DART-MS needs to be sensitive for use in obtaining spectra from microsamples. A spectrum obtained by using a 6.4-mm diameter sample of the bleached kraft paper that contains AKD sizing (ASTM-ISR paper #15) can be compared to a spectrum of the same paper obtained by using an ~10 μg fiber bundle tweezed from the surface of the paper (Fig. 6): the fiber bundle is approximately the size of the period at the end of this sentence. All the peaks needed to identify the paper are present in both temperature-averaged spectra. However, the μg-size sample (Fig. 6b) gives rise to lesser relative abundances of the higher mass products that arise from volatilization of the AKD ketones (m/z values 451–507) in comparison to the lower mass products that arise from thermolysis (m/z values 43–145).

A reasonable explanation for the higher abundances of the AKD ketones from the larger sample is that in the larger sample, more ketones are volatilized from a larger surface area of the paper as compared to the total surface area of the μg-size sample, which is totally charred in the analysis. This can be seen in the photographs in Fig. 6, in which the surface area that is primarily sampled by the helium stream for the larger sample (indicated by the highly darkened surface of the paper in Fig. 6a) is at least five times greater than
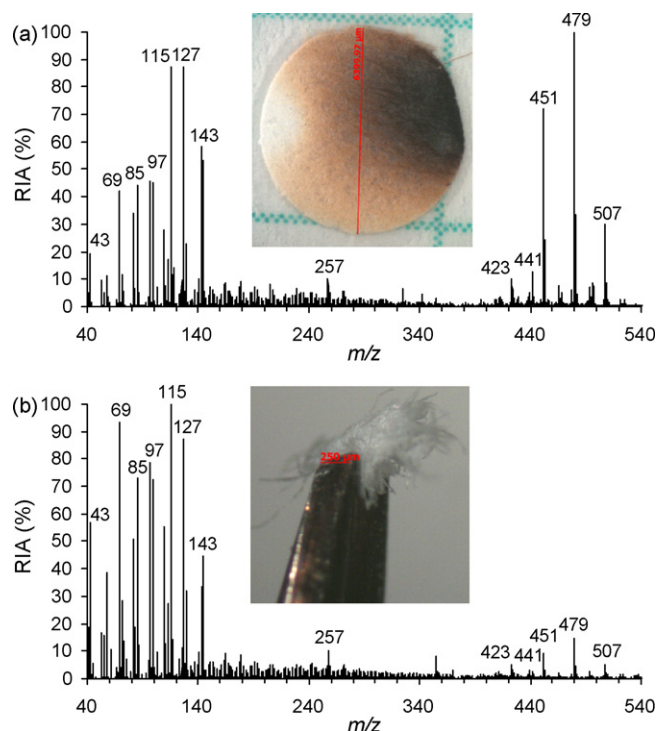
the surface area sampled for the μg-size sample. This could lead to reduced relative abundances of volatilizable components of the paper as opposed to components that arise by thermal degradation of the entire lignocellulose matrix that is contained in a microsample. This is an example, however, of the utility of experiments that incorporate temperature ramping: the spectrum generated from the microsample at ~150 to 250 °C during the ramp is dominated by the products from AKD and is virtually identical to the spectrum shown in Fig. 1b.

3.6. Negative ion DART-MS of reference papers

Negative ion DART-MS spectra of the reference papers are significantly less informative than their positive ion counterparts. Virtually no cellulose ions are observed except for formate, acetate, and a few weakly abundant furan carboxylates that are not detected in the positive ion spectra. Spectra of alum-rosin sized, high-cellulose papers reveal virtually only resin acid anions. Spectra of high-lignin papers primarily show phenolates from coniferaldehyde and the lignin-derived methoxystilbenes. The only extractives that are observed from the SGW papers are the resin acid anions, which make these papers virtually indistinguishable from alum-rosin sized high-cellulose papers.

4. Conclusions

Data presented here show that a series of printing and writing papers can be characterized and differentiated by acquiring their positive ion DART mass spectra across a large temperature range. At lower temperatures, polar organic compounds from rosin, AKD sizing, phytosteroids, and other extractives are volatilized and detected. Higher temperatures primarily result in thermolysis of the lignocellulose matrix that gives rise to cellulose and xylan marker ions, and syringyl (hardwood) and guaiacyl and coumaryl

(softwood) lignin units. Microsamples at least as small as ∼10 μg may be characterized, which means that the method may be used to analyze small paper fragments or fiber bundles sampled from some library and archival collections.

Positive ion DART-MS spectra of lignin-containing papers are closest in similarity to spectra of wood and lignin obtained using in-source and similar direct Py-MS methods. However, ions produced by using positive ion DART-MS are primarily either protonated molecules, resonance-stabilized carbocations that arise from loss of water from protonated alcohols or sterols, or more highly oxidized (unsaturated) species than observed by using Py-MS methods. The DART ionization process may be more efficient and selective at detecting more highly oxidized (particularly conjugated) species present in the papers because they would have higher proton affinities and form more stable $(M+H)^+$ ions. Inorganic salts have no apparent impact on ion formation by DART-MS in contrast to Py-MS. Negative ion DART-MS spectra primarily reveal a few carboxylates and phenolates, which is not enough information to distinguish the papers.

Data presented here have implications beyond the science whose purpose is to preserve library and archival paper collections. DART-MS might be a viable alternative to direct temperature-resolved mass spectrometry (DTMS) in studies of varnishes and oils in historic paintings [56,57]. It might be useful in the pulp and paper industry as an alternative to the time-consuming extraction, derivatization, and chromatographic methods for analyzing organics in wood, pulp, and pulping/bleach liquors, and for monitoring pitch deposits on machinery, in pulp, and in paper mill effluents [58].

The use of positive ion DART-MS to characterize Whatman #1 and the 15 ASTM-ISR reference papers is a prelude to other applications in paper research. Although DART-MS has been used in the forensic community to analyze modern writing inks [22], it has yet to be applied to the analysis of writing inks simultaneously with analysis of the paper matrix. Other research using Py-GC–MS suggests that there may be marker compounds specific for post-consumer recycled paper that may be directly determinable by DART-MS [16]. The spectra of the 16 reference papers analyzed here are benchmarks for the further use of the papers in paper-aging research and in analyzing naturally aged historic papers. In addition, the temperature-averaged spectra are the beginning of the development of a searchable library of DART-MS spectra of printing and writing papers by the Library of Congress that could be of use to researchers in the preservation, pulp, and paper, forensic, and scientific communities at large. These benchmark spectra are the prelude to expanded applications of DART-MS in preservation, forensic, pulp and paper, and other research disciplines.

Acknowledgements

References

[1] R.W. Sindall, The Manufacture of Paper, D. Van Nostrand Co., New York, 1908.
[2] Permanence/durability of the book—vii: physical and chemical properties of book papers, 1507-1949, W. J. Barrow Research Laboratory, Inc., Richmond, 1974.
[3] M.B. Hocking, Handbook of Chemical Technology and Pollution Control, Academic Press, San Diego, 1993, p. 449.
[4] W.E. Scott, Principles of Wet End Chemistry, TAPPI Press, Atlanta, 1996.
[5] R. Boyle, The skeptical chymist: or chymico-physical doubts & paradoxes, touching the spagyrist's principles commonly called hypostatical as they are wont to be proposed and defended by the generality of alchemists, Caldwell & Crooked, London, 1661.
[6] A. Karademir, F. Ozdemir, S. Imamoglu, Effects of alum-rosin sizing on the properties of some wastepaper grades, Biotechnology 6 (2007) 148–152.
[7] Executive Order 13423—Strengthening federal environmental, energy, and transportation management. Federal Register 72 FR 3919, January 26, 2007.
[8] H.J. Porck, Rate of Paper Degradation—The Predictive Value of Artificial Aging Tests, European Commission on Preservation and Access, Amsterdam, 2000.
[9] D. Erhardt, C.S. Tumosa, Chemical degradation of cellulose in paper over 500 years, Restaurateur 26 (2005) 151–158.
[10] M. Missori, M. Righini, Using optical spectroscopy for the study of paper degradation, Gazette due Liver Medieval 49 (2006) 25–35.
[11] A.-L. Dupont, C. Egasse, A. Morin, F. Vasseur, Comprehensive characterization of cellulose- and lignocellulose-degradation products in aged papers: capillary zone electrophoresis of low-molar mass organic acids, carbohydrates, and aromatic lignin derivatives, Carbohydr. Polym. 68 (2007) 1–16.
[12] J. Havermans, Effects of air pollutants on accelerated ageing of cellulose-based materials, Restaurateur 16 (1995) 209–233.
[13] A.S.T.M. Paper Aging Research Program, ASTM Research Report (RR:D06-1004), available as Adjunct to D6789 Standard Test Method for Accelerated Light Aging of Printing and Writing Paper by Xenon-Arc Exposure Apparatus, ASTM International, West Conshohocken, 2002.
[14] L.M. Proniewicz, C. Paluszkiewicz, A. Wesełucha-Birczyńska, A. Barański, D. Dutka, FT-IRE and FT-Raman study of hydro thermally degraded groundwood containing paper, J. Mol. Strict. 614 (2002) 345–353.
[15] T. Trafela, M. Strlič, J. Kolar, D.A. Lichtblau, M. Anders, D.P. Mencigar, B. Pihlar, Nondestructive analysis and dating of historical paper based on ire spectroscopy and chemometric data evaluation, Anal. Chem. 79 (2007) 6319–6323.
[16] T. Yano, H. Ohtani, S. Tsuge, Determination of neutral sizing agents in paper by pyrolysis-gas chromatography, Analyst 117 (1992) 849–852.
[17] G.C. Galletti, P. Bocchini, M.E. Guadalix, G. Almendros, S. Camarero, A.T. Martínez, Pyrolysis products as markers in the chemical characterization of paperboards from waste paper and wheat straw pulps, Biores. Technol. 60 (1997) 51–58.
[18] S. Suzuki, H. Ohi, K. Kuroda, Structural analysis of lignin by pyrolysis-gas chromatography (v), Kari Pa Gikyoushi 51 (1997) 932–944.
[19] C. Laroque, History and analysis of transparent papers, Paper Conserv. 28 (2004) 17–32.
[20] Y. Keheyan, Py/gc/ms analysis of historical papers, BioResource 3 (2008) 829–837.
[21] R.B. Cody, J.A. Laramée, H.D. Durst, Versatile new ion source for the analysis of materials in open air under ambient conditions, Anal. Chem. 77 (2005) 2297–2302.
[22] R.W. Jones, R.B. Cody, J.F. McClelland, Differentiating writing inks using direct analysis in real time mass spectrometry, J. Forensic. Sci. 51 (2006) 915–918.
[23] C.Y. Pierce, J.R. Barr, R.B. Cody, R.G. Massung, A.R. Woolfitt, H. Moura, H.A. Thompson, F.M. Fernandez, Ambient generation of fatty acid methyl ester ions from bacterial whole cells by direct analysis in real time (DART) mass spectrometry, Chem. Commun. (2007) 807–809.
[24] J.Y. Yew, R.B. Cody, E.A. Kravitz, Cuticular hydrocarbon analysis of an awake behaving fly using direct analysis in real-time time-of-flight mass spectrometry, Proc. Natl. Acad. Sci. U.S.A. 105 (2008) 7135–7140.
[25] S.D. Malenknia, T.M. Vail, R.B. Cody, D.O. Sparkman, T.L. Bell, M.A. Adams, Temperature-dependent release of volatile organic compounds of eucalypts by direct analysis in real time (DART) mass spectrometry, Rap. Commun. Mass Spectrom. 23 (2009) 2241–2246.
[26] T. Rothenbacher, W. Schwack, Rapid and nondestructive analysis of phthalic acid esters in toys made of poly(vinyl chloride) by direct analysis in real time single-quadrupole mass spectrometry, Rapid Commun. Mass Spectrom. 23 (2009) 2829–2835.
[27] G.A. Harris, F.M. Fernández, Simulations and experimental investigation of atmospheric transport in an ambient metastable-induced chemical ionization source, Anal. Chem. 81 (2009) 322–329.
[28] L. Song, A.B. Dykstra, H. Yao, J.E. Bartmess, Ionization mechanism of negative ion-direct analysis in real time: a comparative study with negative ion-atmospheric pressure photoionization, J. Am. Soc. Mass Spectrom. 20 (2009) 42–50.
[29] R.B. Cody, Observation of molecular ions and analysis of nonpolar compounds with the direct analysis in real time ion source, Anal. Chem. 81 (2009) 1101–1107.
[30] J.A. Laramée, H.D. Durst, J.M. Nilles, T.R. Connell, An improved protocol for the analysis of alcohols by direct analysis in real time mass spectrometry, Am. Lab. 41 (2009) 25–27.
[31] Z.M. Shabana, Competitive situation of Egyptian cotton in the American market, J. Farm. Econ. 33 (1951) 216–221.
[32] TAPPI T203cm-99. Alpha-, beta- and gamma-cellulose in pulp.
[33] TAPPI T204cm-07. Solvent extractives of wood and pulp.
[34] TAPPI 236 om-06. Kappa number of pulp.
[35] V. Mašura, Relationship between the kappa number and the permanganate number of the western hemlock kraft pulp, TAPPI J. 3 (2004) 9–10.
[36] J. Peng, R. Leone, A.N. Serreqi, C. Breuil, Are Aspen sterols and steryl esters changed structurally by kraft pulping and bleaching? TAPPI J. 82 (1999) 204–211.

[37] H. Hovelstad, I. Leirset, K. Oyaas, A. Fiksdhl, Screening analysis of pinosylvin stilbenes, resin acids, and lignans in Norwegian conifers, Molecules 11 (2006) 103–114.

[38] S.-J. Shin, N.-S. Cho, Y.-Z. Lai, Residual extractives in Aspen kraft pulps and their impact on kappa number and Klason lignin determination, J. Wood Sci. 53 (2007) 494–497.

[39] X. Pan, D. Lachenal, C. Lapierre, B. Monties, V. Neirinch, D. Robert, On the behaviour of spruce thermomechanical pulp lignin during hydrogen peroxide bleaching, Holzforschung 48 (1994) 429–435.

[40] D.G. Mancosky, L.A. Lucia, Use of TOF-SIMS for the analysis of surface metals in H_2O_2-bleached lignocellulosic fibers, Pure Appl. Chem. 73 (2001) 2047–2058.

[41] S.C. Moldoveanu, Analytical Pyrolysis of Natural Organic Polymers, Elsevier, Amsterdam, 1998.

[42] J.J. Boon, I. Pastorova, R.E. Botto, P.W. Arisz, Structural studies of cellulose pyrolysis and cellulose chars by PYMS, PYGCMS, FTIR, NMR and by wet chemical techniques, Biomass Bioenergy 7 (1994) 25–32.

[43] The NIST/EPA/NIH Mass Spectral Library, version 2.0d, build April 26, 2005. Standard Reference Data Program of the National Institute of Standards and Technology, 2005.

[44] ChemSpider. http://www.chemspider.com/ (accessed 14.07.10).

[45] ChemExper. http://www.chemexper.com/ (accessed 14.07.10).

[46] M. Kleen, G. Gellerstedt, Characterization of chemical and mechanical pulps by pyrolysis-gas chromatography/mass spectrometry, J. Anal. Appl. Pyrol. 19 (1991) 139–152.

[47] J.J.C.M. Van Arendonk, G.J. Niemann, J.J. Boon, The effect of enzymatic removal of proteins from plant leaf material as studied by pyrolysis-mass spectrometry: detection of additional protein marker fragment ions, J. Anal. Appl. Pyrol. 42 (1997) 33–51.

[48] R.J. Evans, T.A. Milne, M.N. Soltys, Direct mass-spectrometric studies of the pyrolysis of carbonaceous fuels III. Primary pyrolysis of lignin, J. Anal. Appl. Pyrol. 9 (1986) 207–236.

[49] R. Hempeling, H.-R. Schulten, Chemical characterization of the organic matter in forest soils by curie point pyrolysis-GC/MS and pyrolysis-field ionization mass spectrometry, Org. Geochem. 15 (1990) 131–145.

[50] E.R.E. van der Hage, M.M. Mulder, J.J. Boon, Structural characterization of lignin polymers by temperature-resolved in-source pyrolysis-mass spectrometry and curie-point pyrolysis-gas chromatography/mass spectrometry, J. Anal. Appl. Pyrol. 25 (1993) 149–183.

[51] A. Izumi, K. Kuroda, Pyrolysis-mass spectrometry analysis of dehydrogenation lignin polymers with various syringyl/guaiacyl ratios, Rapid Commun. Mass Spectrom. 11 (1997) 1709–1715.

[52] C. Canevali, M. Orlandi, L. Pardi, B. Rindone, R. Scotti, J. Sipila, F. Morazzoni, Oxidative degradation of monomeric and dimeric phenylpropanoids: reactivity and mechanistic investigation, J. Chem. Soc. Dalton Trans. (2002) 3007–3014.

[53] E.R.E. van der Heijden, J.J. Boon, A combined pyrolysis mass spectrometric and light microscopic study of peatified calluna wood isolated from raised bog peat deposits, Org. Geochem. 22 (1994) 903–919.

[54] E.R.E. van der Hage, J.J. Boon, On-line Curie-point pyrolysis-high-performance liquid chromatographic-mass spectrometric analysis of lignin polymers, J. Chromatogr. A 736 (1996) 61–75.

[55] B.R.T. Simonelt, W.F. Rogge, M.A. Mazurek, L.J. Standley, L.M. Hildemann, G.R. Cass, Lignin pyrolysis products, lignans, and resin acids as specific tracers of plant classes in emissions from biomass combustion, Environ. Sci. Technol. 17 (1993) 2533–2541.

[56] G.A. van der Doelen, K.H. van den Berg, J.J. Boon, Comparative chromatographic and mass–spectrometric studies of triterpenoid varnishes: fresh material and aged samples for paintings, Stud. Conserv. 43 (1998) 249–264.

[57] K. Sutherland, Solvent-extractable components of linseed oil paint films, Stud. Conserv. 48 (2003) 111–135.

[58] A. Rigol, S. Lacorte, D. Barceló, Sample handling and analytical protocols for analysis of resin acids in process waters and effluents from pulp and paper mills, Trends Anal. Chem. 22 (2003) 738–749.